Journal of Alloys and Compounds 514 (2012) 30–34

Contents lists available at SciVerse ScienceDirect

Journal of Alloys and Compounds

journal homepage: www.elsevier.com/locate/jallcom

A new anhydrous bismuth potassium nitrate, $K_3Bi_2(NO_3)_9$: Synthesis, structure characterization and thermal decomposition

A. Goaz[a], V. Uvarov[b,*], I. Popov[b], S. Shenawi-Khalil[a], Y. Sasson[a]

[a] Casali Institute of Applied Chemistry, The Institute of Chemistry, The Hebrew University of Jerusalem, Jerusalem 91904, Israel
[b] The Unit for Nanoscopic Characterization, The Center for Nanoscience and Nanotechnology, The Hebrew University of Jerusalem, Jerusalem 91904, Israel

ARTICLE INFO

Article history:
Received 31 August 2011
Received in revised form 10 October 2011
Accepted 11 October 2011
Available online 7 November 2011

Keywords:
Anhydrous double nitrates
Bismuth nitrates
Thermal decomposition
Rietveld refinement
Ionic radius

ABSTRACT

A new $K_3Bi_2(NO_3)_9$ phase was discovered at a synthesis of Bi-containing photocatalysts. $K_3Bi_2(NO_3)_9$ has cubic structure with unit cell parameter $a = 13.5354(20)$ Å, and belongs to $P4_332$ (No. 212) space group. New phase is isostructural with the $K_3Ln_2(NO_3)_9$ (Ln = La, Ce, Pr, Nd, and Sm) phases. The crystal structure was refined from powder X-ray diffraction (XRD) data. The R_{wp} factor at Rietveld refinement was equal to 8.62%. The morphology of $K_3Bi_2(NO_3)_9$ was characterized using scanning electron microscopy. The value of ionic radius of Bi^{3+} in 12-fold coordination calculated from the unit cell parameter was found to be 1.314(5) Å. $K_3Bi_2(NO_3)_9$ phase and products of its thermal decomposition were studied using XRD, Fourier transform infrared spectroscopy (FTIR) methods and thermal gravimetric analysis (TGA). At 350 °C, $K_3Bi_2(NO_3)_9$ phase was transformed to new unknown intermediate bismuth potassium nitrate that most likely belongs to Sillen type of structure. Geometrical solution for unit cell of this phase was proposed.

1. Introduction

Synthesis of anhydrous double nitrates of the lanthanides with potassium was first reported by Carnall et al. [1]. The synthesized materials have the formula $K_3Ln_2(NO_3)_9$ (Ln = Pr, Nd, Sm, and Er). Crystals were prepared from an eutectic melt of KNO_3, $Ln(NO_3)_3$ and $LiNO_3$ kept at 180 °C for several weeks, and belong to relatively rare cubic $P4_332$ (No. 212) space group or to monoclinic system (when Ln = Er). Later Guillou et al. [2] reported observation of cubic $K_3Ce_2(NO_3)_9$ phase. In this case material was obtained by the evaporation at 313 K of an aqueous solution of cerous nitrate hexahydrate and potassium nitrate. Crystalline structure and thermal properties of anhydrous double lanthanum potassium nitrate $K_3La_2(NO_3)_9$ was reported by Gobichon et al. [3]. Single crystals of $K_2La_2(NO_3)_9$ were obtained from evaporation of a concentrated nitric acid solution of KNO_3 and $La(NO_3)_3{\cdot}6H_2O$ with the molar ratio 3: 2 at room temperature. Syntheses of $Na_3Nd_2(NO_3)_9$, $Rb_3M_2(NO_3)_9$ (M = La, Pr, and Sm) and $(NH_4)_3M_2(NO_3)_9$ (M = La–Gd) with cubic structure were reported by Meyer et al. [4–6]. Until now, published data about properties and structures of double nitrates of potassium and heavy element are rather limited. The infrared and Raman spectral characterization were performed for Pr and Nd salts only [1]. Magnetic susceptibility and paramagnetic resonance were reported in [7–9] for $K_3Nd_2(NO_3)_9$. Chowdhury et al. [10,11] have studied optical properties of $K_3Ln_2(NO_3)_9$ (Ln = Pr, Nd, and Sm) single crystals using low-temperature absorption and circular dichroism spectroscopy. Thermal behaviour and crystal structure of cerous rubidium nitrate $Rb_3Ce_2(NO_3)_9$ were reported by Guillou et al. [12]. Low-temperature X-ray investigation of potassium-neodymium nitrate $K_3Nd_2(NO_3)_9$ was performed and reported by Vigdorchik et al. [14].

In the present work we report about finding of a new crystalline phase $K_3Bi_2(NO_3)_9$ and present its detailed structural, morphological and thermal characterization. We presented here a part of the results obtained under the ongoing experimental study aimed at a development of new Bi-based photocatalysts with using $Bi(NO_3)_3{\cdot}5H_2O$ as source of bismuth. Other new phases discovered in reaction products obtained in due course of this study were reported in [13,15,16]. We believe that that detailed information about structure, morphology, chemical composition and thermal stability of the newly found $K_3Bi_2(NO_3)_9$ phase would be of interest for diverse sections of research community.

2. Experimental

2.1. Synthesis

The material, in which the new $K_3Bi_2(NO_3)_9$ phase has been discovered, has been synthesized by a crystallization from evaporated solution in ambient atmosphere. All the reagents were purchased from Sigma–Aldrich and were used as received without further purification. $Bi(NO_3)_3{\cdot}5H_2O$ (99.0%) (10 mmol) was mixed with distilled water (30 mL) and stirred at room temperature for 20 min. Subsequently, KCl

* Corresponding author.
E-mail address: vladimiru@savion.huji.ac.il (V. Uvarov).

0925-8388/$ – see front matter © 2011 Elsevier B.V. All rights reserved.
doi:10.1016/j.jallcom.2011.10.066

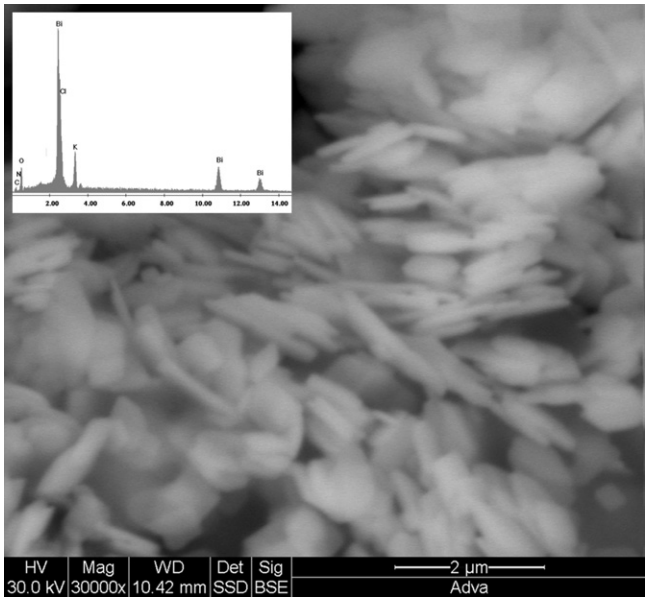

Fig. 1. SEM image and EDS spectrum (inset) of a dry as-synthesized material.

(5 mmol) was added and stirred for 15 min. The slurry was heated in a tube furnace to 200 °C at a heating rate of 1 °C/min, and was kept in this temperature for 2 h. Before loading, the furnace was pre-heated to 100 °C. A white powder was obtained.

2.2. Material characterization

X-ray diffraction data were collected with D8 Advance diffractometer (Bruker AXS, Karlsruhe, Germany) with Göbel Mirror parallel-beam optics. XRD patterns from 5° to 90° 2θ were recorded at room temperature using CuKα radiation (λ = 0.15418 nm) with following measurement conditions: step scan mode with a step size 0.02° 2θ and counting time of 1 s per step for preliminary study and 12 s per step for structural refinement. TOPAS-v.3 [17] software was used for structure refinement.

Morphological observations and chemical analysis were performed with environmental scanning electron microscope (ESEM) Quanta 200 (FEI Company, Netherlands) equipped with EDS detector (EDAX-TSL, USA). Pure β-Bi_2O_3 (Aldrich) was used for justification of standardless quantification procedure applied to EDS data. FTIR spectra were acquired with APLPA-P Module (Bruker Optics GmbH) with diamond ATR object. For the thermal gravimetric analysis Mettler TC10A/TC15 TA controller and Mettler M3 thermobalance (Greifensee, Switzerland) were used. Samples of 20–25 mg were weighed and heated to 25–700 °C at a rate of 2 °C/min.

3. Results and discussion

Fig. 1 shows SEM image and energy-dispersive (EDS) spectrum acquired at a dry as-synthesized material. Under back-scattered electrons (BSEs) imaging the powder is a mixture of micron-size bright regions with well-defined flake-morphology and darker regions without clear morphological features. This result indicates inhomogeneous distribution of chemical elements through the observed powder. According to EDS analysis, the material consists of Bi, K, Cl, N and O. Therefore, we suggest that bright flakes should be enriched by heavier Bi as compared to darker phase in which enrichment with K, N and O may be expected.

Careful examination of an XRD pattern obtained from a powder specimen reveals that the specimen contains two crystalline phases. The first phase is known BiOCl (PDF 01-73-2060). Peak's positions and intensity of the second phase well correspond to the same for a $K_3Pr_2(NO_3)_9$ phase (PDF 04-09-6738). The unit cell parameter *a* of cubic phase was about 13.53 Å. Therefore we have assumed that the synthesized phase is Bi-structural analog of a $K_3Pr_2(NO_3)_9$ phase. Indeed, both elements have 3^+ active valence, and many cases of Bi-lanthanides substitution in crystal structures were reported [15,18–20]. Following this primary finding, we tried to synthesize a pure $K_3Bi_2(NO_3)_9$ phase, but our attempts were not successful. Addition of a distilled water and a subsequent drying at a room temperature lead to formation of bismuth nitrates. Minor change in synthesis conditions resulted in formation of K–Bi–O–N phases of Sillen-type with tetragonal or orthorhombic structure. We suggest therefore that a window of conditions for preparation of a pure potassium-bismuth nitrate from used components is very narrow. Therefore for detailed characterization and Rietveld structural refinement we chose a two-phase sample (as-synthesized) containing $K_3Bi_2(NO_3)_9$ and BiOCl. Taking into account the aforesaid $K_3Pr_2(NO_3)_9$ structure has been chosen as base model at structure refinement. We wish to note here that although $K_3Pr_2(NO_3)_9$, $K_3Nd_2(NO_3)_9$ and $K_3Sm_2(NO_3)_9$ phases are attributed to $P4_332$ (No. 212) space group, its counterparts $K_3Ce_2(NO_3)_9$ and $K_3La_2(NO_3)_9$ are both attributed to $P4_132$ (No. 213) group. The $P4_332$ (No. 212) and $P4_132$ (No. 213) space groups are enantiomorphic space groups and cannot be distinguished based on XRD spectra. Therefore we use original attribution of $K_3Pr_2(NO_3)_9$ to $P4_332$ (No. 212) space group in our model.

The graphical result of Rietveld structural refinement is shown in Fig. 2. Site occupancy factors for all atoms were fixed. Preferred orientation was corrected using the spherical harmonics method [21]. The data were corrected for peak asymmetry due to axial divergence [22]. Each of the refined parameter was accepted only if it was physically meaningful. The final refined structural parameters and selected bond distances are given in Tables 1–3. Full Rietveld refinement report (with full set of bond lengths and bond angles) for $K_3Bi_2(NO_3)_9$ is resulted in Supplementary material.

The values of bond lengths and bond angles resulted in Table 3 are in good agreement with the earlier published results for

Table 1
Crystallographic data for $K_3Bi_2(NO_3)_9$.

Color	White
Empirical formula	$K_3Bi_2(NO_3)_9$
Crystal data	
Crystal system	Cubic
Space group	$P4_332$ (No. 212)
Lattice parameters *a* (Å)	13.5354(20)
Volume (Å^3)	2479.8(11)
Formula units, *Z*	4
Density (g/cm^3)	2.9284(13)
Structural refinement	
Software	TOPAS v.3
Diffractometer	Bruker D8 Advance
2θ range	5–90
No. of reflections (theoretical)	128
No. of data points	4250
No. of structural parameters	28
No. of refined parameters	37
Background function	Chebyshev polynomial
Profile function	Pseudo-Voigt
R_{exp} (%)	6.23
R_{wp} (%)	8.62
R_p (%)	6.71
Goodness of fit	1.38

Table 2
Refined atomic coordinates for $K_3Bi_2(NO_3)_9$.

Site	Atom	*x*	*y*	*z*	Occ.	B_{eq} (Å^{-2})
K (12*d*)	K^{1+}	0.125	0.3116(6)	−0.0616(6)	1	1.09(9)
Bi (8*c*)	Bi^{3+}	0.2999(4)	0.2999(4)	0.2999(4)	1	1.11(3)
N1 (12*d*)	N^{5+}	0.4869(5)	−0.2369(5)	0.125	1	0.7(3)
O1 (24*e*)	O^{2-}	0.4010(4)	0.7460(3)	0.0806(4)	1	1.9(2)
O2 (12*d*)	O^{2-}	0.5509(4)	−0.3009(4)	0.125	1	1.8(2)
N2 (24*e*)	N^{5+}	0.3876(6)	0.1645(6)	0.1475(8)	1	1.4(4)
O3 (24*e*)	O^{2-}	0.3112(3)	0.1406(4)	0.1979(6)	1	1.9(2)
O4 (24*e*)	O^{2-}	0.4272(5)	0.1071(4)	0.0899(3)	1	1.9(2)
O5 (24*e*)	O^{2-}	0.4255(5)	0.2466(4)	0.1664(6)	1	1.8(2)

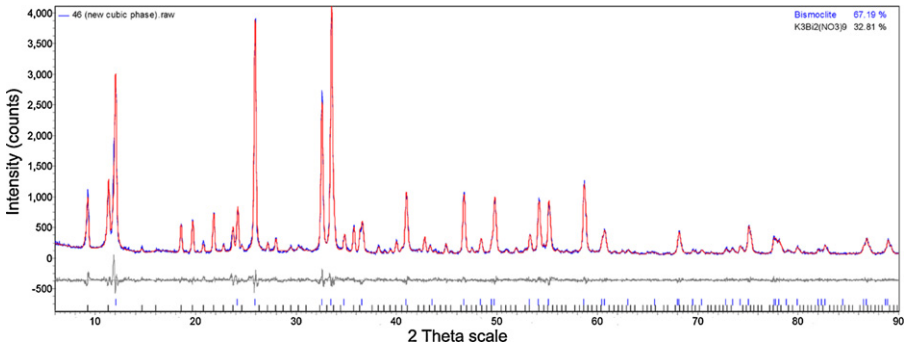

Fig. 2. Graphical representation of Rietveld refinement results for the sample containing BiOCl and new $K_3Bi_2(NO_3)_9$ phase. Peak positions of BiOCl and $K_3Bi_2(NO_3)_9$ are shown by vertical bars (upper and lower, respectively).

Table 3
Selected bond lengths and bond angles for $K_3Bi_2(NO_3)_9$.

Bond lengths (Å)			
Bi–O1	2.768(4)	O3–O4	2.191(9)
Bi–O2	2.640(5)	N1–O1	1.329(5)
Bi–O3	2.565(6)	N1–O2	1.224(9)
Bi–O5	2.584(7)	N2–O3	1.280(1)
K–O4	2.809(6)	N2–O4	1.220(1)
O1–O2	2.209(8)	N2–O5	1.250(1)
Bond angles (°)			
O1–N1–O1	119.7(4)	O3–N2–O5	116.6(8)
O1–N1–O2	120.5(4)	O4–N2–O5	121.0(8)
O3–N2–O4	122.2(8)		

$K_3Ln_2(NO_3)_9$ [1]. The fragment of $K_3Bi_2(NO_3)_9$ structure is shown in Fig. 3. The atomic arrangement is practically identical to that described in detail in [1,3]. The Bi^{3+} cations are situated in center of a somewhat distorted icosahedron and are surrounded by twelve oxygen atoms belonging to nitrate groups (with the short Bi–O3 (2.565(6) Å) and long Bi–O1 (2.768(4) Å) distances). The nitrate groups have two different configurations, and the geometry of NO_3 anions slightly deviates from the regular triangle. In nitrate group of the first type (N1) every oxygen atom is bonded to Bi atoms.

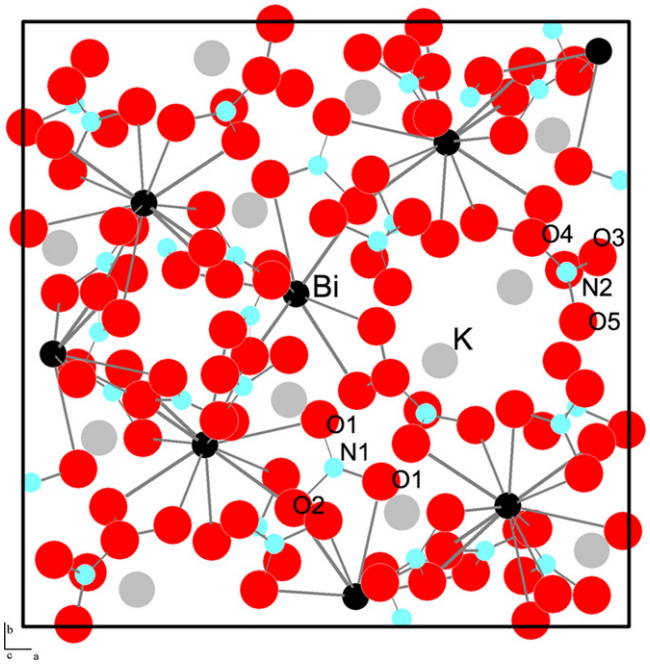

Fig. 3. The fragment of $K_3Bi_2(NO_3)_9$ structure (the view along its *c*-axis).

The O(2) atom simultaneously belongs to two bismuth atoms and is thereby bridging, while the two other O(1) atoms are divided between Bi and K. In the second type nitrate groups, two oxygen atoms O(3) and O(5) are bound to one Bi atom, while O(4) atom is bound exclusively with K atoms. The obtained values of bond lengths and bond angles for the nitrate group are close to published data [1,2].

The structure parameters (unit cell parameter *a* and Bi–O bond distances) obtained for the new phase $K_3Bi_2(NO_3)_9$ allow to calculate ionic radius of Bi^{3+} in 12-fold coordination. The previously published data for its value differs substantially. Gomah-Pettry et al. [23] reported on value 1.3 Å, Xue et al. [24] – 1.03 Å, Jayaprakash and Shanker [25] – 0.855 Å and Padmini and Kutty [26] – 1.29 Å. Unfortunately these results were obtained for crystalline phases, in which bismuth was located on sites with the mixed occupation. Based on the reported structural data on $K_3Ln(NO_3)_9$ family phases, we analyzed a relationship between the values of unit cell parameters and the ionic radii of lanthanides (La, Ce, Pr, Nd and Sm). In Fig. 4a we show this relation graphically by using the values of ionic radii published in Table 5-2 [27]. The linear dependence of ionic radius on unit cell parameter *a* is obvious, and could be described by a linear regression equation $R_i = 0.3968a - 4.0564$ (where R_i is an ionic radius and *a* is an unit cell parameter). Substitution of *a* parameter value obtained for the new $K_3Bi_2(NO_3)_9$ phase (13.535(2) Å) to the equation above we get the value of 1.314(2) Å for ionic radius of Bi^{3+} in 12-fold coordination. This value is close to the data published in [23]. Shannon [28] has shown that almost linear relation exists between coordination number and a value of ionic radius. Fig. 4b shows that calculated value of ionic radius is in a good agreement with this rule.

The FTIR spectrum acquired from the tested material is shown in Fig. 5. Six IR active modes arising from the NO_3^- vibrations are observed. These IR frequencies at 736.7 cm^{-1}, 803.5 cm^{-1}, 1030.3 cm^{-1}, 1297 cm^{-1} and 1433.6 cm^{-1} fits well to the data reported by Carnall et al. [1] for $K_3Pr_2(NO_3)_9$ and by Bünzli et al. [30] for nitrate groups in anhydrous lanthanide nitrates and oxynitrates. A specific fine structure of strips is clearly seen in a spectrum. According to [30] the fine structure of the lower frequency bands at 1297 cm^{-1}, 803.5 cm^{-1} and 736.7 cm^{-1} is very sensitive to the dryness of the nitrates; it disappears when the salts get hydrated. The presence of this fine structure of the strips confirms, therefore, an anhydrous character of synthesized phase. The vibration in the absorption region between 250 cm^{-1} and 600 cm^{-1}, is typical of the cubic structure of the oxides [30]. Group of vibrational frequencies in 500 cm^{-1} region can be attributed to BiOCl phase [31]. For comparison we show the FTIR spectrum of a pure BiOCl phase in Supplementary materials (Fig. S1).

Fig. 6 shows TGA results obtained for the two-phase sample containing BiOCl and the new $K_3Bi_2(NO_3)_9$ phases. We also

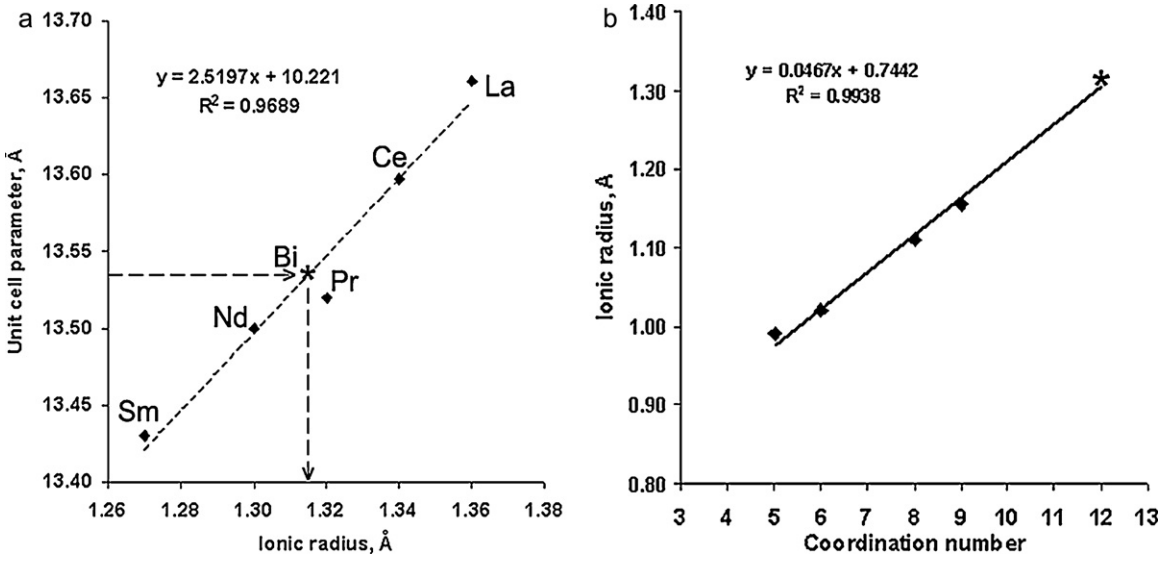

Fig. 4. (a) Values of ionic radii *vs* unit cell parameter *a* for cubic $K_3Ln(NO_3)_9$ phases (adopted from [27]); (b) values of Bi^{3+} ionic radii *vs* coordination number of Bi^{3+} (adopted from [28] (Bi^{3+} ionic radius in 9-coordination adopted from [29])). Calculated value of ionic radius of Bi^{3+} in 12-coordination is labeled by asterisk.

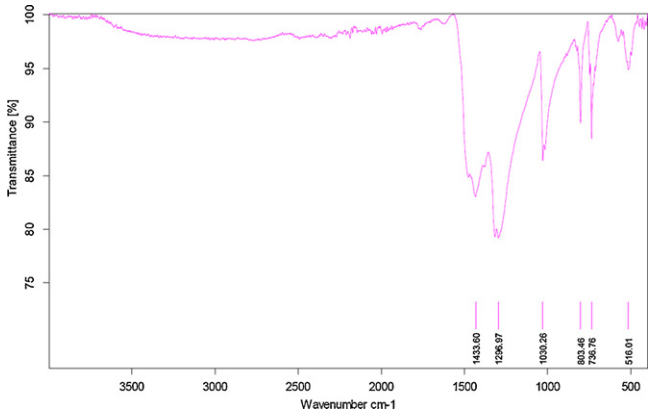

Fig. 5. FTIR spectrum of as-synthesized material containing two phases: BiOCl and the new $K_3Bi_2(NO_3)_9$.

acquired TGA curve from a pure BiOCl at the same heating conditions (shown in Supplementary materials, Fig. S2). A pure BiOCl exhibited no weight losses up to 750 °C that coincides with the previously reported data [29]. In contrast, the two-phase sample underwent weight losses under heating to 250–350, 450–550 and 650–700 °C. These weight losses could be caused by transformations occurred in new. Earlier thermal decomposition of hydrated and anhydrous double potassium lanthanum nitrates was studied in detail by Gobichon et al. [3]. They reported that the decomposition of the pure phase $K_3La_2(NO_3)_9$ up to 600 °C takes place with the successive formation of X_α, X_β, and also cubic La_2O_3. These conclusions were confirmed by temperature-dependent X-ray powder diffraction study and differential scanning calorimetry. It is clear our results are in good agreement with these data.

In order to identify the transformations observed at thermal analysis, we heated the two-phase sample to the temperatures in which sufficient weight losses were detected (at 350 °C and 700 °C) and then analyzed heat treated samples using XRD and FTIR methods. The results of this experiment are shown in Fig. 7 and in Supplementary material. As is seen in Fig. 7b, after heating to 350 °C for 30 min, peaks of $K_3Bi_2(NO_3)_9$ phase disappeared, while peaks of BiOCl remained practically unchanged as compared to the pattern obtained from the as-synthesized powder (Fig. 7a). We identified a peak at 23.65° 2θ as the strongest reflection of a KNO_3 that indicates the presence of KNO_3 traces in the sample heated to 350 °C. Suggesting the presence of only one more crystalline phase in the heat treated material, we indexed all other unidentified reflections

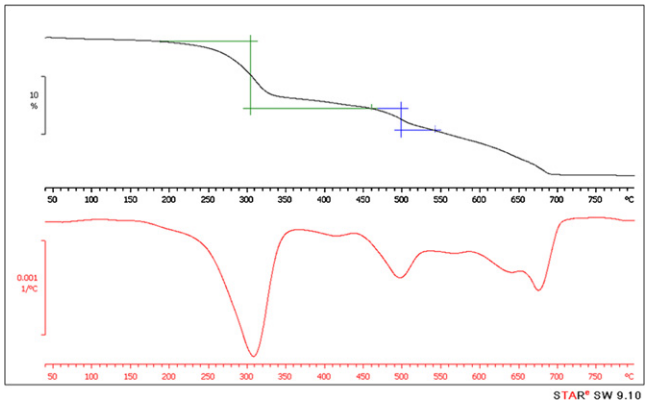

Fig. 6. TGA curve obtained at heating of two-phase sample (BiOCl and $K_3Bi_2(NO_3)_9$) up to 750 °C. Upper and lower curves represent TGA curve and its first derivative, respectively.

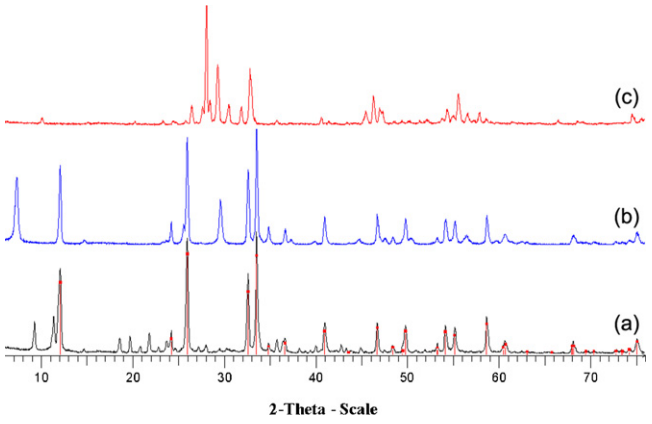

Fig. 7. XRD patterns acquired from: (a) as-synthesized two-phase material (BiOCl and $K_3Bi_2(NO_3)_9$); (b) two-phase material heat treated at 350 °C for 30 min; and (c) two-phase material heat treated at 700 °C for 30 min. Peak's positions of BiOCl are labeled.

(from the phase obtained at thermal decomposition) with using the Crysfire software [32]. Two of the suggested geometric solutions with the highest figure of merits were obtained: (i) a tetragonal body-centered cell with $a = 3.87$ Å and $c = 24.11$ Å (F20 = 43.3), and (ii) an orthorhombic body-centered unit cell with $a = 3.86$ Å, $b = 3.87$ Å and $c = 24.12$ Å (F20 = 34.5). Both solutions are obtained with use of Treor 90 utility [33]. These solutions are almost geometrically equivalent and cannot be distinguished using conventional XRD data. By comparing these possible geometrical solutions with the published data about the crystalline structure of similar chemical compounds [34–38], we conclude that the additional *X*-phase formed at 350 °C is most likely belongs to Sillen type of structure. The main feature of these phases is the presence of the metal-oxygen ($[Bi_2O_2]^{2+}$) layers in their structure, and halogen atoms or other atomic groups are located between these layers. It is necessary to note that the FTIR spectrum of the sample heated at $T = 350$ °C was very similar to that obtained from the as-synthesized sample (see Supplementary material, Fig. S3). Therefore we conclude that the additional phase appearing under heating of an initial phase mixture of BiOCl and $K_3Bi_2(NO_3)_9$ is most probably potassium bismuth nitrate. Detailed studying of crystal structure of this phase will be continued. Thus, the phase transformation at 350 °C of $K_3Bi_2(NO_3)_9$ could occur by following scheme:

$$K_3Bi_2(NO_3)_9 + BiOCl \xrightarrow{\text{heating at } 350\,^\circ C} X\text{-phase} + BiOCl \quad (1)$$

In order to emphasize that the heated material contains a BiOCl, which does not change at this temperature, we have written BiOCl both on the left and right sides of this equation. The proposed transformation is very similar to reported by Gobichon et al. [3] for potassium lanthanum nitrate.

As well as we may conclude, this transformation occurred within the new $K_3Bi_2(NO_3)_9$ phase only, while BiOCl phase remained beyond this reaction. The proposed transformation is very similar to reported by Gobichon et al. [3] for potassium lanthanum nitrate.

As is seen in Fig. 7c, at heating to 700 °C for 30 min a phase mixture of BiOCl and $K_3Bi_2(NO_3)_9$ was completely converted into four crystalline phases: β-Bi_2O_3 (PDF 73-6885), $Bi_{12}O_{17}Cl_2$ (PDF 37-0702), KCl (PDF 02-4543) and $Bi_{12.8}O_{19.2}$ (PDF 81-0563). The concentration of KCl by results of the semi-quantitative XRD analysis was about 15.2%. This corresponds to the total 8 wt% potassium concentration that fits well the results of EDS analysis of the initial as-synthesized material. Thus, the transformations occurring at 700 °C can be described as:

$$K_3Bi_2(NO_3)_9 + BiOCl \xrightarrow{\text{annealing at } 700\,^\circ C} \beta\text{-}Bi_2O_3 + Bi_{12}O_{17}Cl_2 + KCl + Bi_{12.8}O_{19.2} \quad (2)$$

We conclude that unlike a low-temperature process occurring at 350 °C, the high temperature decomposition of 700 °C completely destroys both co-existing phases of the as-synthesized material.

4. Conclusion

$K_3Bi_2(NO_3)_9$ phase was observed for the first time and is the structure analog of the $K_3Ln_2(NO_3)_9$ (*Ln* = La, Ce, Pr, Nd, and Sm) phases. In spite of the fact that we no succeeded to obtain the pure $K_3Bi_2(NO_3)_9$, its structure has been successfully refined from powder XRD data and its thermal behaviour has been studied. Employing the structural similarity between the $K_3Bi_2(NO_3)_9$ and the known anhydrous double potassium lanthanide nitrates, we calculated the value of ionic radius of Bi^{3+} in 12-fold configuration. It was found to be 1.314(2) Å. By applying TGA, we found that the new $K_3Bi_2(NO_3)_9$ phase was unstable under heating from room temperature up to 750 °C. Products of its thermal decomposition were identified by XRD analysis, and geometrical solutions for new unknown low temperature intermediate bismuth potassium nitrate (*X*-phase) were proposed. Obtained FTIR and TGA results are in good agreement with previously reported data for anhydrous double nitrates of the lanthanides.

We hope the article can be of interest to our colleagues working in the area of Bi-based photocatalysts with using $Bi(NO_3)_3{\cdot}5H_2O$ as source of bismuth.

Further details of the crystal structure investigation can be obtained from the Fachinformationszentrum Karlsruhe, 76344 Eggenstein-Leopoldshafen, Germany (crysdata@fiz.karlsruhe.de) on quoting the depository number CSD-422618.

Appendix A. Supplementary data

Supplementary data associated with this article can be found, in the online version, at doi:10.1016/j.jallcom.2011.10.066.

References

[1] W.T. Carnall, S. Siegel, J.R. Ferraro, B. Tanil, E. Gebert, Inorg. Chem. 12 (1973) 560–564.
[2] N. Guillou, J.P. Auffredic, D. Louer, Acta Crystallogr. C 51 (1995) 1032–1034.
[3] A.-E. Gobichon, J.-P. Auffrédic, D. Louër, J. Solid State Chem. 144 (1999) 68–80.
[4] E. Manek, G. Meyer, Eur. J. Solid State Inorg. Chem. 30 (1993) 883–894.
[5] S. Stockhause, G. Meyer, Z. Kristallogr, New Cryst. Struct. 212 (1997) 316.
[6] E. Manek, G. Meyer, Z. Anorg. Allg. Chem. 616 (1992) 141–144.
[7] G. Luo, L.R. Corruccini, Solid State Commun. 128 (2004) 251–254.
[8] G. Luo, L.R. Corruccini, J. Magn. Magn. Mater. 278 (2004) 359–366.
[9] G. Luo, L.R. Corruccini, J. Phys. Chem. Solids 67 (2006) 639–642.
[10] P.K. Chatterjee, A. Nath, D. Nath, M. Chowdhury, Chem. Phys. Lett. 110 (1984) 95–98.
[11] M. Chowdhury, A.K. Banerjee, T. Kundu, L. Kundu, T. Chakraborty, Proc. Indian Acad. Sci. (Chem. Sci.) 102 (1990) 255–268.
[12] N. Guillou, J.P. Auufredic, D. Louer, J. Solid State Chem. 122 (1996) 59–67.
[13] S. Shenawi-Khalil, Y. Kritsman, E. Menes, V. Uvarov, I. Popov, Y. Sasson, Catal. Commun. 12 (2011) 1136–1141.
[14] A.G. Vigdorchik, Y.A. Malinovskii, A.G. Dryuchko, I.A. Verin, Sov. Phys. Crystallogr. 37 (1992) 466–469.
[15] V. Uvarov, S. Shenawi-Khalil, I. Popov, J. Solid State Chem. 183 (2010) 1484–1489.
[16] A. Goaz, V. Uvarov, D.O. Charkin, S. Shenawi-Khalil, I. Popov, V.A. Dolgikh, Y.Sasson, Solid State Sci. (2011), doi:10.1016/j.solidstatesciences.2011.11.017.
[17] TOPAS V3, General Profile and Structure Analysis Software for Powder Diffraction Data, User's Manual, Bruker AXS, Karlsruhe, Germany, 2003.
[18] M. Devillers, F. De Smet, O. Tirions, Thermochim. Acta 260 (1995) 165–185.
[19] A.B. Missyul, E.M. Khairullina, I.A. Zvereva, Glass Phys. Chem. 36 (2010) 247–250.
[20] J. Ting, B.J. Kennedy, R.L. Withers, M. Avdeev, J. Solid State Chem. 182 (2009) 836–840.
[21] M. Järvinen, J. Appl. Crystallogr. 26 (1993) 525–531.
[22] L.W. Finger, D.E. Cox, A.P. Jephcoat, J. Appl. Crystallogr. 27 (1994) 892–900.
[23] J.R. Gomah-Pettry, A.N. Salak, P. Marchet, V.M. Ferreira, J.P. Mercurio, Phys. Stat. Sol. (B) 241 (2004) 1949–1956.
[24] L.A. Xue, Y. Chen, R.J. Brook, Mater. Sci. Eng. B 1 (1988) 193–201.
[25] R. Jayaprakash, J. Shanker, Physica C 205 (1993) 377–382.
[26] P. Padmini, T.R.N. Kutty, J. Mater. Sci. Mater. Electron. 5 (1994) 203–209.
[27] V. S. Sastri, J.-C. G. Bünzli, V. R. Rao, G. V. S. Rayudu, J. R.,Perumareddi, Modern Aspects of Rare Earths and Complexes, Elsevier, Amsterdam, 2003, p.378.
[28] R.D. Shannon, Acta Crystallogr. A 32 (1976) 751–767.
[29] R.L. Frost, A.R. McKinnon, P.A. Williams, K.L. Erickson, M.L. Weier, P. Leverett, Neues Jb. Miner. Abh. 181 (2005) 11–19.
[30] J.-C.G. Bünzli, E. Moret, J.-R. Yersin, Helv. Chim. Acta 61 (1978) 762–771.
[31] Z.-T. Deng, F.-Q. Tang, A.J. Muscat, Nanotechnology 19 (2008) 295705–295711.
[32] R. Shirley, The Crysfire 2002 System for Automatic Powder Indexing: User's Manual, The Lattice Press, 41 Guildford Park Avenue, Guildford, Surrey GU2 7NL, England, 2002, Available at: http://www.ccp14.ac.uk/tutorial/crys/.
[33] P.-E. Werner, L. Eriksson, M. Westdahl, J. Appl. Crystallogr. 18 (1985) 367–370.
[34] V.A. Dolgikh, L.N. Kholodkovskaya, Russ. J. Inorg. Chem. 37 (1992) 488–502.
[35] L.G. Sillén, Naturwissenschaften 30 (1942) 318–324.
[36] B. Aurivillius, Arkiv fur Kemi 1 (1949) 499–512.
[37] D.O. Charkin, P.S. Berdonosov, V.A. Dolgikh, P. Lightfoot, J. Solid State Chem. 175 (2003) 316–321.
[38] A. Snedden, D.O. Charkin, V.A. Dolgikh, P. Lightfoot, J. Solid State Chem. 178 (2005) 180–184.